Inhalation treatment of primary lung cancer using liposomal curcumin dry powder inhalers

CrossMark

Tongtong Zhang[a,b], Yanming Chen[b,c], Yuanyuan Ge[a,b], Yuzhen Hu[a,b], Miao Li[a], Yiguang Jin[a,b,*]

[a]Department of Pharmaceutical Sciences, Beijing Institute of Radiation Medicine, Beijing 100850, China
[b]Anhui Medical University, Hefei 230001, China
[c]China Pharmaceutical University, Nanjing 210009, China

Abstract Lung cancer is the leading cause of cancer-related deaths. Traditional chemotherapy causes serious toxicity due to the wide bodily distribution of these drugs. Curcumin is a potential anticancer agent but its low water solubility, poor bioavailability and rapid metabolism significantly limits clinical applications. Here we developed a liposomal curcumin dry powder inhaler (LCD) for inhalation treatment of primary lung cancer. LCDs were obtained from curcumin liposomes after freeze-drying. The LCDs had a mass mean aerodynamic diameter of 5.81 μm and a fine particle fraction of 46.71%, suitable for pulmonary delivery. The uptake of curcumin liposomes by human lung cancer A549 cells was markedly greater and faster than that of free curcumin. The high cytotoxicity on A549 cells and the low cytotoxicity of curcumin liposomes on normal human bronchial BEAS-2B epithelial cells yielded a high selection index partly due to increased cell apoptosis. Curcumin powders, LCDs and gemcitabine were directly sprayed into the lungs of rats with lung cancer through the trachea. LCDs showed higher anticancer effects than the other two medications with regard to pathology and the expression of many cancer-related markers including VEGF, malondialdehyde, TNF-α, caspase-3 and BCL-2. LCDs are a promising medication for inhalation treatment of lung cancer with high therapeutic efficiency.

1. Introduction

Lung cancer is one of leading causes of morbidity and mortality among all malignant tumors worldwide. The major causes of lung cancer include smoke, air pollution and ionizing radiation[1]. Small-cell lung cancer (15%–20%) and non-small-cell lung cancer (NSCLC, 80%–85%) are the main types of lung cancer[2,3]. Clinical treatments of primary lung cancer mainly include surgery, radiotherapy and chemotherapy. Chemotherapeutics are commonly combined with the other two treatments. However, oral or injection administration of anticancer drugs, the most commonly applied clinical treatment, results in whole-body exposure to the toxic agents, leading to low drug concentrations in tumor tissues and unwanted drug distribution into normal tissues. In this traditional chemotherapy, serious adverse effects and low therapeutic efficiencies are usually unavoidable[4]. Therefore, the targeted or local delivery of drugs to increase drug concentration in tumor tissues and decrease drug in normal tissues is emergent for the treatment of cancer including lung cancer[5].

Pulmonary drug delivery is a noninvasive administration method by inhalation or spraying through the throat and branchillea. Inhalation therapy is efficient treatment of lung diseases such as asthma, pneumonia and chronic obstructive pulmonary disease (COPD) due to direct drug delivery into the lung[6,7]. Dry powder inhalers (DPIs) are portable solid powder delivery units without propellants. DPIs can directly target drugs into the deep sites of the lung[8]. The stability of loaded drugs is usually better in DPIs than in aerosols and nebulizers[9]. Our previous research demonstrated that oridonin-loaded large porous microparticles had a strong anti-lung cancer effect after pulmonary delivery[10]. Liposomes are phospholipid vesicles that can entrap hydrophobic drugs in their bilayer or hydrophilic drugs in the interior water phase. Liposomes are an efficient formulation for the treatment of cancer because they can enhance drug entry into cells. Generally, intravenous injection of liposomes is the major route of administration[11]. Recently, liposomes have been used for pulmonary delivery to treat lung diseases such as pneumonia[12].

Curcumin is isolated from *Curcuma longa*. It is one of the most studied and most popular natural products of the past decade. Curcumin has been demonstrated to have extensive pharmacological activities including antioxidation[13], anti-inflammation[14–16], anticancer[17], antimicrobial[18], and immunoregulation.[19] Curcumin inhibits the proliferation and migration of A549 lung cancer cells and enhances apoptosis[20,21]. However, curcumin shows low water solubility, poor bioavailability and rapid *in vivo* metabolism[22–24], which seriously limits its clinical applications. A variety of nanotechnologies have been tried to modify the physicochemical properties of curcumin and its distribution *in vivo*[25,26]. However, these technologies remain at the laboratory level without further clinical applications. Nonetheless, topical curcumin formulations may be a good strategy for local treatment of diseases because the major physicochemical disadvantages of curcumin may be avoided[27,28].

In this study, we prepared curcumin liposomes and liposomal curcumin dry powder inhalers (LCDs) for inhalation treatment of primary lung cancer *via* pulmonary delivery. The lung deposition of LCDs was evaluated. The therapeutic efficiency and mechanism of LCDs were explored on rat lung cancer models with comparison to curcumin powders and gemcitabine (a clinical first-line anticancer drug).

2. Materials and methods

2.1. Materials

Curcumin was provided by Sinopharm Reagent Co., Ltd. (Shanghai, China). Soybean lecithin (SPC > 90%) and cholesterol were purchased from Shanghai Taiwei Medicine Co., Ltd. (China) and Sinopharm Reagent Co., Ltd. (Shanghai, China), respectively. Gemcitabine was provided by Jiangsu Hansoh Pharmaceutical Co., Ltd., China. 3-Methylcholanthrene (MCA, TRC, USA), diethylnitrosamine (DEN, Tokyo Chemical Industry, Japan) and iodized oil (Guerbet, French) were used for generating rat primary lung cancer models. All other chemicals and solvents were of analytical grade or high performance liquid chromatographic (HPLC) grade. Pure water prepared with the Heal Force Pure Water System and was always used.

2.2. Animals

Male Sprague–Dawley (SD) rats (190–200 g) were provided by the Beijing Institute of Radiation Medicine (BIRM, Beijing, China). Handling and surgery were according to the Laboratory Animals' Guiding Principles. Lung bronchoalveolar lavage fluids (BALFs) were collected. The lung tissues were excised and then stained with hematoxylin and eosin (H&E).

2.3. Preparation of liposomal curcumin dry powder inhalers

Curcumin-loaded conventional liposomes were prepared by a film method. Briefly, curcumin and the lipids including SPC and cholesterol (5:1, mol/mol) were dissolved in 5 mL of tetrahydrofuran and placed in a round-bottom flask. The solvent was removed under vacuum to obtain a thin film that was hydrated with a phosphate buffered solution (PBS, pH 7.0) at 37 °C for 1 h at 200 rpm (Thermostatic Air Vibrator, THZ-D, Taicang Experimental Instrument Factory, Suzhou, China). Mannitol was added to the liposomes which were further freeze-dried in a lyophilizer (LGJ-30F, Beijing Songyuan Huaxing Technology Develop Co., Ltd., China) for 36 h to obtain liposomal curcumin dry powder inhalers (LCDs).

2.4. Measurement of encapsulation and loading efficiencies in liposomes

Free curcumin was separated from curcumin liposomes by centrifugation at 10,000 rpm (High Speed Centrifuge, TGL-16B, Shanghai Anting Scientific Instrument Factory, Shanghai, China) for 10 min. The supernatant was filtered through a 0.45-μm filter. Free curcumin in the filtrate was analyzed with an HPLC system (Angilent 1260, US): a Dikma Diamonsil C18 column (250 mm × 4.6 mm, 5 μm), a detection wavelength of 425 nm and a mobile phase of acetonitrile/water/acetic acid (60:39:1, *v/v*) at a flow rate of 1 mL/min. Total curcumin was also determined after the LCDs were completely dissolved in ethanol. Encapsulated curcumin was calculated from total curcumin minus free curcumin. The curcumin encapsulation efficiency (EE) and loading efficiency (LE) were calculated with Eqs. (1) and (2).

$$EE\ (\%) = \frac{\text{Encapsulated curcumin}}{\text{Total curcumin}} \times 100\% \qquad (1)$$

$$LE\ (\%) = \frac{\text{Total curcumin}}{\text{LCDs}} \times 100\% \qquad (2)$$

2.5. Characterization of inhaled powders

Two inhaled powders were characterized. Surface morphologies of curcumin powders (CPs) and LCDs were observed with a scanning electron microscope (SEM, S-4800, Hitachi, Japan). LCDs were further rehydrated and observed with a Hitachi H-7965 80-kV transmission electron microscope (TEM) after negative staining with 2% sodium phosphotungstate solutions. The initial curcumin liposomes were used as a control. A dynamic light scattering method was used to measure the sizes and size distribution of liposomes with Zetasizer Nano ZS (Malvern, UK).

The repose angles of CPs and LCDs were measured by the fixed funnel method[29]. Tapped densities were calculated with the graduated flask method. The volume diameters were measured with a particle size analyzer (BT2001, Bettersize Instruments Ltd., Dandong, China). The mass mean aerodynamic diameter (MMAD) of powders was calculated with Eq. (3).

$$D_a = D_g \sqrt{\frac{\rho}{\rho_0 \chi}} \qquad (3)$$

where D_a is the MMAD; D_g is the geometric mean diameter and is equal to the volume diameter when the 50% particle volume (less than a certain volume diameter) are determined; ρ is the tapped density (g/cm^3); ρ_0 is the standard density (1 g/cm^3); and χ is the dynamic shape factor (here, $\chi = 1$).

2.6. Simulated lung deposition

In vitro simulated lung deposition of CPs and LCDs was determined using a Next Generation Impactor (NGI, Copley, Nottinggham, UK). The fine particle fraction (FPF, $<5\,\mu m$) was calculated with Eq. (4) [30].

$$FPF = \frac{\text{Drugs in stages } 2-7}{\text{Drugs in all stages}} \times 100\% \qquad (4)$$

2.7. Cytotoxicity

The cytotoxic assays of curcumin, curcumin liposomes and gemcitabine against normal human bronchial epithelial cells (BEAS-2B, provided by Z. Yang from BIRM) and human lung cancer A549 cells (provided by Chinese Academy of Medical Sciences, China) were performed with CCK-8 kits (Gen-View Scientific Inc., USA). Cells were seeded at a density of 5×10^5 cells/well and incubated at 37 °C for 24 h. Curcumin was dissolved in a small volume of dimethyl sulphoxide (DMSO) and then diluted with the HLC-8 culture media and the DMEM culture media (Gibco, USA) for use with BEAS-2B and A549 cells, respectively, where DMSO was less than 0.1% in the final dilutions. LCDs and gemcitabine were also dispersed in the above culture media. A series of drug concentrations, including 6.25, 12.5, 25, 50 and 100 μmol/L of curcumin or gemcitabine, were tested for cytotoxicity. The cells were incubated with these dilutions for 24 h. The CCK-8 reagents were added into the wells and then incubated for 4 h. They were measured at 450 nm using a microplate reader (ELX800, BioTek Instrument, Inc, USA). Cell viability was calculated as (absorbance of sample)/(absorbance of control)×100%. The selection index is defined as the viability ratio of A549/BEAS-2B.

2.8. Evaluation of cell uptake

Cellular uptake of CPs and LCDs was investigated on A549 cells. Briefly, a sterilized cover glass of 20 mm × 20 mm was put in the wells of 6-well plates. A549 cells were seeded on glass with a density of 5×10^5 cells/well and incubated for 24 h at 37 °C. The cells were treated with the above dilutions (containing 100 μmol/L curcumin) of CPs or LCDs. At the predetermined time points, the cover glass was washed 3 times with PBS (pH 7.0), fixed with 4% paraformaldehyde solution for 15 min, and then washed 3 times again with PBS. The cells were stained with 4′,6′-diamidino-2-phenylindole (DAPI) for 30 min. Qualitative assay of cell uptake was performed using a confocal laser scanning microscope (CLSM, UltraVIEW VOX, PerkinElmer, USA) at the excitation wavelength of 488 nm.

2.9. Hoechst 33258 nucleus staining

The process of Hoechst 33258 nuclear staining of A549 cells was almost the same as the above cell uptake experiment except for Hoeschst 33258 (5 μg/mL) staining for 20 min. The slides were examined by fluorescent microscopy at the excitation wavelength of 330–380 nm and the emission wavelength of 420 nm.

2.10. Flow cytometry

A549 cells were seeded in the wells of 6-well plates with a density of 5×10^5 cells/well and incubated for 24 h at 37 °C. The dilutions (containing 100 μmol/L curcumin) of CPs or LCDs were added and co-incubated for 12 h. The apoptosis of A549 cells was detected with flow cytometry on a fluorescence-activated cell sorting (FACS) caliber (Becton-Dickinson) and apoptotic cells were identified with an annexin V-FITC/PI kit (Neobioscence Technology Co., Ltd., China). The ratios of annexin V+/PI− and V+/PI+ regions were calculated with CellQuest software, indicating the rates of early- and late-stage apoptosis, respectively.

2.11. Pharmacodynamic study

Rat primary lung cancer models were prepared following pulmonary delivery of MCA and DEN in our laboratory[10]. The chemical-induced lung cancer models served as a good simulation of clinical NSCLC induced by toxic agents. Healthy rats and tumor-bearing rats were administered saline (0.2 mL) by spraying saline into the lungs through the trachea with a long soft plastic tube. CPs (1 mg each rat) and LCDs (10 mg each rat, containing 1 mg curcumin) were sprayed into the lungs of tumor-bearing rats using an insufflator (DP-4M, Penn-Century Inc., USA) through the trachea without anesthesia. Gemcitabine solutions (0.1 mL, 10 mg/mL) in saline were also sprayed into the lungs of tumor-bearing rats with a soft plastic tube. All the medications were administered once a day for 4 days, after which the rats were sacrificed and the trachea exposed. The right lung was ligated using a hemostatic clamp. The left lung was flushed with cold saline (4 °C, 4 mL, flushing three times). The acquired BALFs were centrifuged at 3500 rpm (Low Speed Centrifuge, DT5-4B, Beijing Shidai Beili Centrifuge Co., Ltd., Beijing, China) for 15 min and the supernatant was collected for detection of cytokines or markers.

2.12. Histopathological examination

The upper lobe of the right lung was immersed in 10% formalin solutions and then embedded in paraffin. The pathological sections were prepared, stained with H&E, and observed under a microscope.

2.13. Immunohistochemistry

The upper lobe of the right lungs was processed as mentioned above. The tissues embedded in paraffin were deparaffined in xylene and rehydrated with ethanol. The tissues were immersed in the ethylenediamine tetraacetic acid (EDTA) antigen retrieval solutions (pH 8.0) and the antigens were removed after microwave heating for 15 min. The sample was washed with water for 5 min and processed with a hydrogen peroxide solution (3%, 30 μL) to remove the endogenous peroxidases. The primary antibody of vascular endothelial growth factor (VEGF) diluted with PBS (pH 7.4) was applied and incubated for 30 min at room temperature. The secondary antibody to the primary antibody was applied for 30 min at room temperature with interval PBS washing. Immunohistochemical detection was performed following the kit instructions. The stained sections were observed under a microscope (BDS200-FL, Chongqing Optec Instrument Co., Ltd., China).

2.14. ELISA measurements

Tumor necrosis factor-α (TNF-α), malondialdehyde (MDA) and caspase-3 are the important markers reflecting immune responses, oxidation and apoptosis, respectively[31]. The concentration of TNF-α in the BALFs was measured with the corresponding enzyme-linked immunosorbent assay (ELISA) kits and caspase-3 in the lung cancer tissues was measured using a caspase-3 activity assay kit (KeyGEN BioTECH Corp., China). MDA in the lung cancer tissues was measured with an MDA assay kit (Nanjing Jiancheng Bioengineering Institute, China).

2.15. Western blot measurements

TNF-α, BCL-2 and pro-caspase-3 in the lung tissues were measured according to our previous research[10]. Briefly, the proteins in the lung tissues were extracted and collected by centrifugation. Quantification of these proteins was performed using a BCA kit (CWBIO,

China). TNF-α, BCL-2 and pro-caspase-3 proteins were separated by SDS-PAGE and then visualized after a series of immunohistochemical processes. The proteins were quantified using the ImageJ software (the National Institutes of Health, US).

2.16. Statistical analysis

All data are expressed as means $\pm$ standard deviations (SDs). One-way ANOVA was performed for all statistical evaluations. Individual differences between groups were identified using an LSD test. Statistical significance was defined as a P value <0.05 or <0.01.

3. Results and discussion

3.1. Characteristics of inhaled powders and curcumin liposomes

Liposomal curcumin suspensions were stable yellow homogeneous liquids (Fig. 1A). Both LCDs and CPs were yellow powders (Fig. 1B). The SEM images showed the cylinder crystals (Fig. 1C) of free curcumin and the irregular microparticles (less than 20 μm in diameter, Fig. 1D) of LCDs. The DLS results showed that the curcumin liposomes rehydrated from LCDs were very small (94.65 ± 22.01 nm) with a narrow size distribution (PDI, 0.26 ± 0.01). The TEM images further demonstrated that both the initial curcumin liposomes and the reconstructed curcumin liposomes appeared as homogenous spherical vesicles (Fig. 1E and F). Therefore, LCDs can easily transform into curcumin liposomes in the lung after pulmonary delivery. It is known that liposomes are good drug carriers that facilitate drug entry into cells. Therefore, the liposomal formulation of curcumin should enhance its pharmacological activity.

The particulate properties of LCDs and CPs were different. The reposes were similar, $15.46 \pm 1.41°$ and $17.44 \pm 1.35°$ ($n=3$) for LCDs and CPs, respectively. However, they showed different D_{50} of 15.02 ± 0.12 μm and 22.21 ± 0.62 μm for LCDs and CPs,
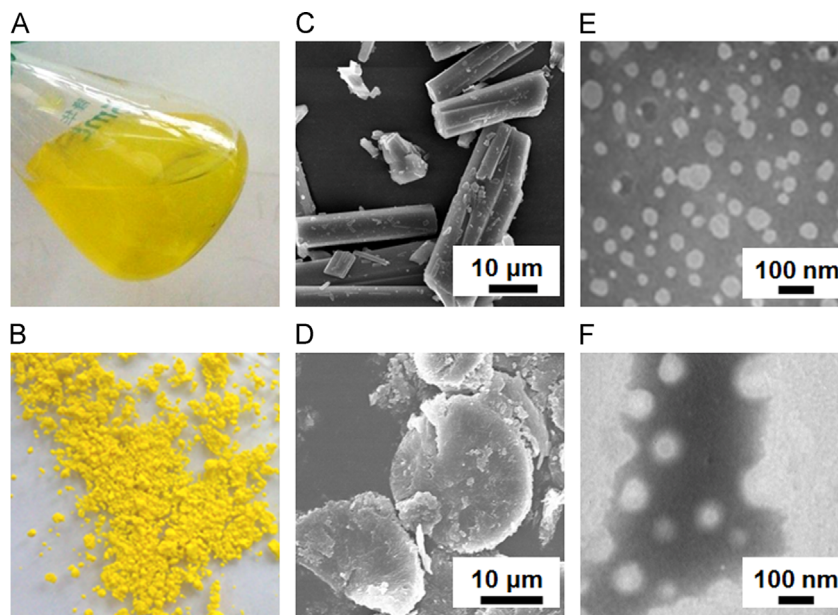

Figure 1 Appearances and morphologies of inhaled powders and curcumin liposomes. Appearances of curcumin liposomes (A) and LCDs (B). SEM images of CPs (C) and LCDs (D). TEM images of the initial curcumin liposomes (E) and the curcumin liposomes rehydrated from LCDs (F).
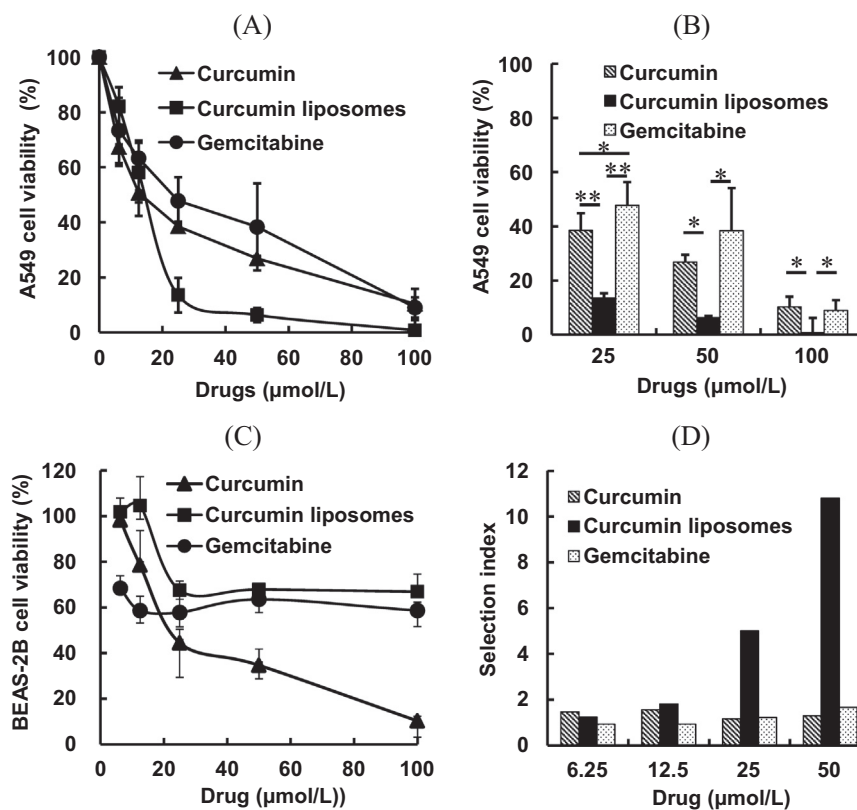
Figure 2 Viabilities of A549 (A, B) and BEAS-2B (C) cells after treatment with curcumin, curcumin liposomes and gemcitabine ($n=4$), and selection indexes (D) of these regimens. $^*P<0.05$; $^{**}P<0.01$.

respectively. Furthermore, the tapped densities of LCDs and CPs were 0.16 ± 0.01 g/cm^3 and 0.36 ± 0.01 g/cm^3, respectively, *i.e.*, LCDs were much looser than CPs. The MMAD of LCDs and CPs were 5.81 ± 0.06 and 13.32 ± 0.36 μm, respectively. The fine particle fraction (FPF) of LCDs was $46.71\pm5.23\%$. Therefore, LCDs are more suitable for pulmonary inhalation than CPs due to the high lung deposition of LCDs.

3.2. High in vitro anti-lung cancer effect and selection index of curcumin liposomes

Free curcumin, curcumin liposomes (reconstructed from LCDs) and gemcitabine showed similar anti-A549 cell effects at a low concentration (*e.g.*, 20 μmol/L) with viabilities of $58.08\pm8.32\%$, $50.65\pm10.91\%$ and $63.26\pm6.50\%$ at 12.5 μmol/L, respectively. However, when the drug concentrations were increased to more than 20 μmol/L, the anticancer effects of the medications showed great differences (Fig. 2A). For example, when the drug concentrations were 25 μmol/L, curcumin liposomes had a low A549 cell viability of $13.50\pm1.79\%$; but free curcumin and gemcitabine only lowered cell viabilities to $38.48\pm6.34\%$ and $47.80\pm8.57\%$, respectively. Furthermore, when the drug concentrations were up to 50 μmol/L, the cell viabilities were $26.86\pm2.58\%$, $6.28\pm0.62\%$ and $38.82\pm15.83\%$ for free curcumin, curcumin liposomes and gemcitabine, respectively (Fig. 2B). Therefore, curcumin shows high *in vitro* anti-lung cancer cell effect, even better than the clinical first-line anticancer drug, gemcitabine. Other reports also show the high anticancer effect of curcumin[32,33]. Liposomes efficiently enhance the anticancer activity of curcumin possibly by improving the permeability of curcumin and increasing the uptake of cells.
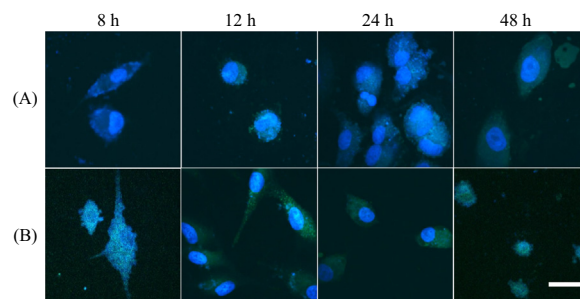

Figure 3 CLSM images of the A549 cells incubated with CPs (A) and LCDs (B) at different incubation times. The scale bar indicates 25 μm.

The cytotoxicity on BEAS-2B was also determined. Curcumin and curcumin liposomes showed little cytotoxicity when the curcumin concentrations were less than 10 μmol/L[34,35], but gemcitabine had a higher cytotoxicity within the same concentration range (Fig. 4C). After the drug concentrations exceeded 25 μmol/L, all of them showed strong inhibition of cell growth. Curcumin liposomes and gemcitabine maintained a stable cell viability of about 60% up to 100 μmol/L, but curcumin showed continually increasing inhibition with increased concentrations. In the culture process, we found that curcumin precipitated in the wells and some yellow crystals appeared. Therefore, we speculate that the crystals of curcumin could affect the growth of BEAS-2B cells, which is enhanced with the increase of added curcumin. On the other hand, liposomal curcumin does not precipitate due to the formulation. Curcumin liposomes had large selection indexes much higher than free curcumin and gemcitabine when the concentration was over 25 μmol/L (Fig. 4D). At 50 μmol/L, the selection indexes of

curcumin, curcumin liposomes and gemcitabine were 1.29, 10.81 and 1.66, respectively, and at $100\,\mu mol/L$, the selection indexes changed to 0.99, 92.47 and 6.52, respectively. Therefore, LCD would appear to be a very safe and highly effective inhalable medication for treatment of lung cancer compared to inhaled curcumin and gemcitabine.

3.3. High endocytosis efficiency of curcumin liposomes

Free curcumin and curcumin liposomes showed differing endocytosis into A549 lung cancer cells according to the CLSM results (Fig. 3). Almost no curcumin was internalized in the cells regardless of whether free curcumin or curcumin liposomes were co-incubated with A549 cells for 8 h. However, 12 h later, significant green fluorescence appeared in the plasma of cells treated with curcumin liposomes due to the considerable internalization of curcumin. In comparison, little green fluorescence appeared in the plasma of cells treated with free curcumin. The phenomena at 24 h were unchanged. Forty-eight hours later, the curcumin liposome-treated cells shrank and the nuclei were almost dissolved, indicating strong cell apoptosis. However, the free curcumin-treated cells survived well with some curcumin internalization post-48 h. The large difference in endocytosis between free curcumin and curcumin liposomes can be ascribed to the water-insoluble property of curcumin and the high dispersion and permeability of liposomes. Therefore, curcumin liposomes are readily taken up by cells and increase the apoptosis of cancer cells. In other reports, liposomes are well known to improve drug permeability into cells[36].

3.4. Improved cell apoptosis by curcumin liposomes

Hoechst staining is used for detection of cell nucleus damage[37]. The number of A549 cells significantly decreased and some of the nuclei were bright due to condensation after treatment with curcumin liposomes for 12 h (Fig. 4B), indicating that the nuclei were highly damaged. The condensation of cell nuclei shows that apoptosis takes place[38]. In contrast, the free curcumin-treated A549 cells did not show significant changes at the same time (Fig. 4A). Therefore, curcumin liposomes enhanced cell apoptosis mainly resulting from the improved cell uptake of curcumin, which was in consistent with the above cell uptake results. Finally, few cells remained after treatment with curcumin liposomes for 48 h. Furthermore, the flow cytometric results also showed the strongly improved apoptosis effect of curcumin liposomes compared to free curcumin (Fig. 4C). Apoptosis rates in the cells treated with curcumin liposomes or free curcumin were 13.3% and 6.9% after 12 h incubation, respectively.

3.5. High anticancer effect of curcumin liposomes

The in vivo pharmacodynamic study further showed the anti-lung cancer effects of the medications after pulmonary delivery. Numerous tumor nodes and bleeding appeared in the lungs of the rat lung cancer models (Fig. 5b, Lung) compared with the smooth lung surfaces of healthy rats (Fig. 5a, Lung), indicating acute damage in lung cancer tissues. After administration of CPs, the tumor nodes and bleeding in the lung remarkably decreased compared to the tumor-bearing lung (Fig. 5c, Lung). Moreover, the tumor nodes and bleeding in the LCD and gemcitabine groups hardly appeared and the lungs even showed a similar appearance to the lung of healthy rats (Fig. 5d, e, Lung).

The pathological sections further showed the details of lung cancer and treatments (Fig. 5). Cell proliferation was well shown in the tumor-bearing lung (Fig. 5, H&E). After administration of CPs, LCDs and gemcitabine, cell proliferation was highly inhibited due to possible apoptosis of cancer cells,
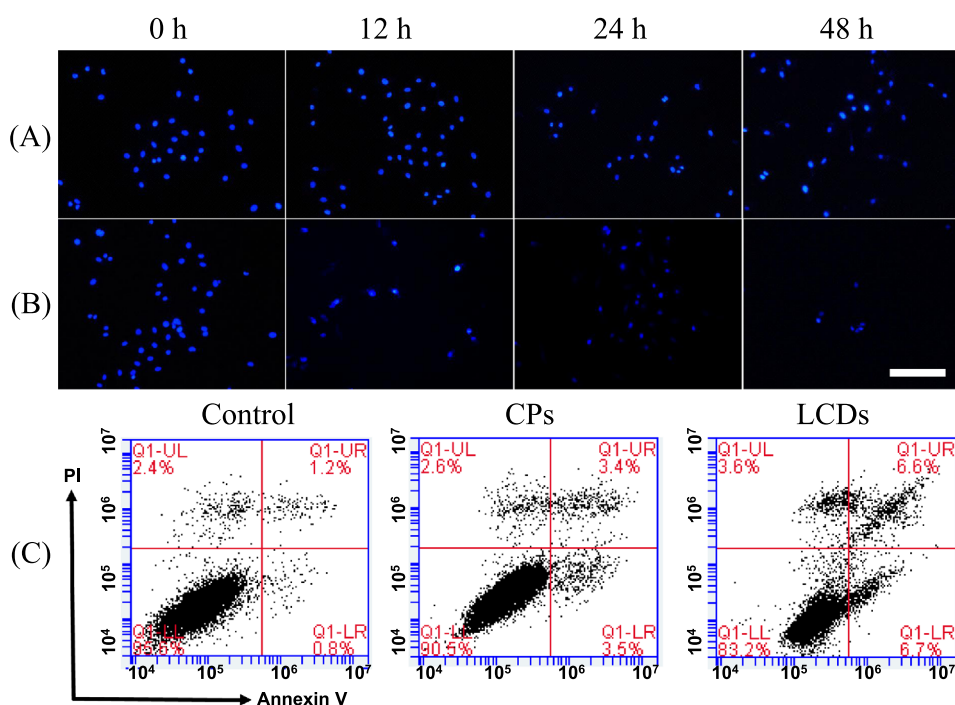

Figure 4 Images of Hoechst-stained A549 cells after treatment with CPs (A) and LCDs (B), and flow cytometric graphs (C). The scale bar indicates $100\,\mu m$.
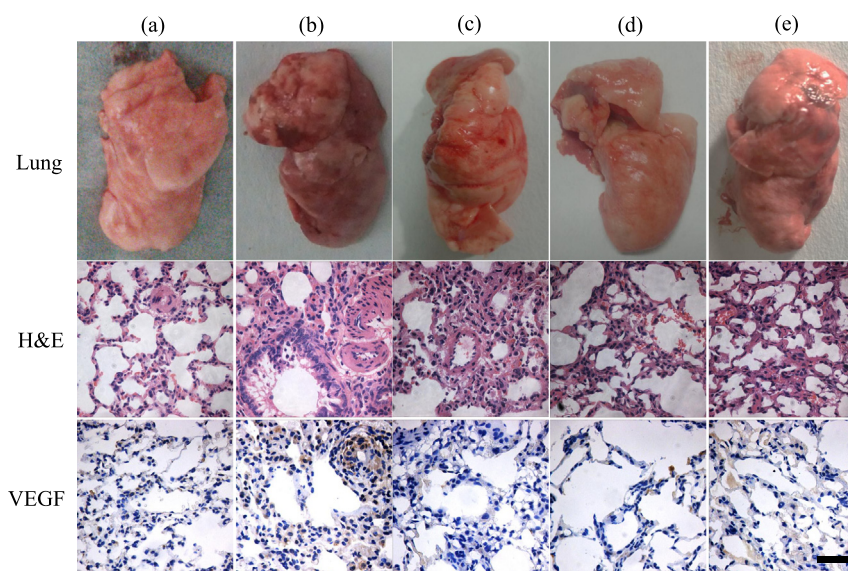
Figure 5 Appearances of lungs, and images of lung tissue sections (400 ×) and VEGF expression (400 ×) from the healthy rats (a); the lung cancer rats (b); the lung cancer rats treated with CPs (c); the lung cancer rats treated with LCDs (d); and the lung cancer rats treated with gemcitabine (e). The scale bars indicate 100 μm.

wherein the anti-proliferation effect of LCDs was strongest (Fig. 5d, H&E).

VEGF can improve the growth of blood vessels during tumor progression and invasion. VEGF is demonstrated to be highly expressed in many types of tumors[39]. In this study, the tissues from primary lung cancer showed high VEGF expression compared to normal lung tissues (Fig. 5a, b, VEGF). After administration of CPs, LCDs and gemcitabine, the VEGF expressions were highly inhibited, wherein the anti-VEGF effect of LCDs was strongest (Fig. 5d, VEGF). Therefore, the inhalable LCD is a potent anti-primary lung cancer medication *via* pulmonary delivery.

3.6. High anti-oxidation effect of curcumin liposomes

The carcinogenic chemicals used in this study have strong cytotoxicity and can cause local lung injuries. Curcumin is known to have strong anti-inflammatory and anti-oxidant effects[40–43]. Malondialdehyde (MDA) is a typical oxidation indicator[44]. Curcumin was reported as a potent antioxidant to decrease MDA[45]. In this study, the lung tissues of tumor-bearing rats showed high MDA levels (Fig. 6A). All the medications decreased the MDA levels. Moreover, the MDA levels in the CP and LCD groups showed statistical differences ($P < 0.05$) compared to those of rat lung cancer models, wherein the effect of LCDs was strongest. However, gemcitabine had no effect on lung MDA.

3.7. High anti-inflammatory effect of curcumin liposomes

Lung cancer can stimulate the innate immune system, leading to the extensive expression of pro-inflammatory cytokines[46]. TNF-α is an important pro-inflammatory cytokine[47]. TNF-α levels in the three treatment groups decreased remarkably as shown by the ELISA and western blot assays (Fig. 6B and E). Furthermore,

LCDs had the strongest ability to decrease TNF-α, even much higher than gemcitabine ($P < 0.01$, Fig. 6B). More importantly, the TNF-α level in the LCD group was very close to that in the healthy rats ($P = 0.496$) (Fig. 6B and E). Therefore, curcumin has an anti-inflammatory effect in the treatment of primary lung cancer, and liposomes can enhance the effect of curcumin.

3.8. Strong apoptosis effect of curcumin liposomes

Caspase-3 is an important protein to improve apoptosis[48]. In this study, all the medications enhanced the expression of caspase-3 (Fig. 6C), wherein the effect of LCDs was highest with a significant statistical difference ($P < 0.01$) compared to the lung cancer model (Fig. 6C). Moreover, the levels of pro-caspase-3 showed the same profile as the expression of caspase-3 (Fig. 6E). Pro-caspase-3 is the precursor of caspase-3, which plays a key role in the caspase-3 pathway[49]. Therefore, it is concluded that curcumin has a high anti-lung cancer effect and enhanced apoptosis is a major reason. Furthermore, liposomes improve the apoptosis effect of curcumin by enhancing its permeability and cell endocytosis.

Rapid proliferation of lung cancer cells in lung cancer usually follows the expression of anti-apoptosis proteins[50,51]. BCL-2 is a protein that inhibits apoptosis. It prevents the release of cytochrome C in the mitochondria to inhibit apoptosis[52]. Here, three medications including free curcumin, curcumin liposomes and gemcitabine inhibited the expression of BCL-2 in lung tissue (Fig. 6D and E). However, only LCDs showed a significant decrease of BCL-2 expression ($P < 0.05$) in comparison to the lung cancer model.

4. Conclusions

We report the application of curcumin for inhalation treatment of primary lung cancer. Curcumin is a widely-active pharmacological agent extracted from plants. Its anticancer effects are well
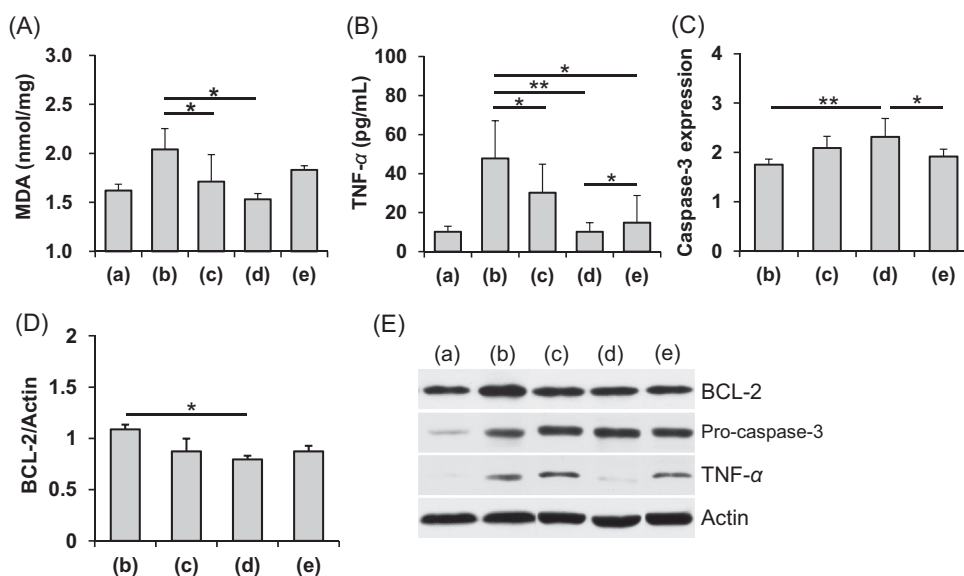
Figure 6 Effects of the medications on the oxidation indicator (MDA, A) pro-inflammatory cytokine (TNF-α, B), and apoptosis (caspase-3, C; BCL-2, D) ($n=6$). $^*P<0.05$; $^{**}P<0.01$. Protein expression by Western blot (BCL-2, pro-caspase3 and TNF-α, E). The meanings of (a)–(e) are described in Fig. 5.

documented. However, the poor stability, low water solubility, low bioavailability, and rapid metabolism of curcumin seriously limit its biomedical applications. In this study, curcumin and its liposomal formulation were directly administered to the lungs of rats with lung cancer *via* pulmonary delivery, where the bioavailability and metabolism limitations of curcumin do not exist. Furthermore, our investigation of the anti-lung cancer mechanisms of curcumin demonstrates that the strong anti-oxidative and anti-inflammatory effects and the improvement in apoptosis induced by curcumin significantly contribute to its anticancer effect. More importantly, the liposomal formulation highly enhances the effect of curcumin by overcoming the water solubility limit and increasing cell endocytosis. This inhalable liposomal curcumin formulation is a promising pulmonary medication for the treatment of lung cancer.

References

1. Liu R, Wei S, Chen J, Xu S. Mesenchymal stem cells in lung cancer tumor microenvironment: their biological properties, influence on tumor growth and therapeutic implications. *Cancer Lett* 2014;**353**:145–52.
2. Chen Y, Li J, Chen S, Zhang Y, Hu Y, Zhang G, et al. Nab-paclitaxel in combination with cisplatin *versus* docetaxel plus cisplatin as first-line therapy in non-small cell lung cancer. *Sci Rep* 2017;**7**:10760–7.
3. Wang K, Chen M, Wu W. Analysis of microRNA (miRNA) expression profiles reveals 11 key biomarkers associated with non-small cell lung cancer. *World J Surg Oncol* 2017;**15**:175–80.
4. Jin J, Hu K, Zhou Y, Li W. Clinical utility of the modified Glasgow prognostic score in lung cancer: a meta-analysis. *PLoS One* 2017;**12**: e0184412.
5. Shen H, Wang L, Chen W, Menard K, Hong Y, Tian Y, et al. Tissue distribution and tumor uptake of folate receptor–targeted epothilone folate conjugate, BMS-753493, in CD2F1 mice after systemic administration. *Acta Pharm Sin B* 2016;**6**:460–7.
6. Yang MY, Chan JGY, Chan H-K. Pulmonary drug delivery by powder aerosols. *J Control Release* 2014;**193**:228–40.
7. Kuzmov A, Minko T. Nanotechnology approaches for inhalation treatment of lung diseases. *J Control Release* 2015;**219**:500–18.
8. Debnath SK, Saisivam S, Omri A. PLGA ethionamide nanoparticles for pulmonary delivery: development and *in vivo* evaluation of dry powder inhaler. *J Pharm Biomed Anal* 2017;**145**:854–9.
9. Ungaro F, d'Angelo I, Coletta C, d'Emmanuele di Villa Bianca R, Sorrentino R, Perfetto B, et al. Dry powders based on PLGA nanoparticles for pulmonary delivery of antibiotics: modulation of encapsulation efficiency, release rate and lung deposition pattern by hydrophilic polymers. *J Control Release* 2012;**157**:149–59.
10. Zhu L, Li M, Liu X, Du L, Jin Y. Inhalable oridonin-loaded poly(lactic-*co*-glycolic)acid large porous microparticles for *in situ* treatment of primary non-small cell lung cancer. *Acta Pharm Sin B* 2017;**7**:80–90.
11. Sen K, Mandal M. Second generation liposomal cancer therapeutics: transition from laboratory to clinic. *Int J Pharm* 2013;**448**:28–43.
12. Li M, Zhang T, Zhu L, Wang R, Jin Y. Liposomal andrographolide dry powder inhalers for treatment of bacterial pneumonia *via* anti-inflammatory pathway. *Int J Pharm* 2017;**528**:163–71.
13. Jaroonwitchawan T, Chaicharoenaudomrung N, Namkaew J, Noisa P. Curcumin attenuates paraquat-induced cell death in human neuroblastoma cells through modulating oxidative stress and autophagy. *Neurosci Lett* 2017;**66**:40–7.
14. Priyanka A, Shyni GL, Anupama N, Salin Raj P, Anusree SS, Raghu KG. Development of insulin resistance through sprouting of inflammatory markers during hypoxia in 3T3-L1 adipocytes and amelioration with curcumin. *Eur J Pharmacol* 2017;**812**:73–81.
15. Dewangan AK, Perumal Y, Pavurala N, Chopra K, Mazumder S. Preparation, characterization and anti-inflammatory effects of curcumin loaded carboxymethyl cellulose acetate butyrate nanoparticles on adjuvant induced arthritis in rats. *J Drug Del Sci Tech* 2017;**41**: 269–279.
16. Gan Y, Zheng S, Baak JPA, Zhao S, Zheng Y, Luo N, et al. Prediction of the anti-inflammatory mechanisms of curcumin by module-based protein interaction network analysis. *Acta Pharm Sin B* 2015 590–5.
17. Mirzaei H, Naseri G, Rezaee R, Mohammadi M, Banikazemi Z, Mirzaei HR, et al. Curcumin: a new candidate for melanoma therapy?. *Int J Cancer* 2016;**139**:1683–95.
18. Chen J, He Z-M, Wang F-L, Zhang Z-S, Liu X-z, Zhai D-D, et al. Curcumin and its promise as an anticancer drug: an analysis of its anticancer and antifungal effects in cancer and associated complications from invasive fungal infections. *Eur J Pharmacol* 2016;**772**:33–42.
19. Seyedzadeh MH, Safari Z, Zare A, Navashenaq JG, Razavi sA, Kardar GA, et al. Study of curcumin immunomodulatory effects on reactive astrocyte cell function. *Int Immunopharmacol* 2014;**22**:230–5.

20. Lee W-H, Loo C-Y, Ong H-X, Traini D, Young PM, Rohanizadeh R. Synthesis and characterization of inhalable flavonoid nanoparticle for lung cancer cell targeting. *J Biomed Nanotechnol* 2015;**11**:1–16.

21. Wan K, Sun L, Hu X, Yan Z, Zhang Y, Zhang X, et al. Novel nanoemulsion based lipid nanosystems for favorable *in vitro* and *in vivo* characteristics of curcumin. *Int J Pharm* 2016;**504**:80–8.

22. Hu L, Kong D, Hu Q, Gao N, Pang S. Evaluation of high-performance curcumin nanocrystals for pulmonary drug delivery both *in vitro* and *in vivo*. *Nanoscale Res Lett* 2015;**10**:381–9.

23. El-Sherbiny IM, Smyth HDC. Controlled release pulmonary administration of curcumin using swellable biocompatible microparticles. *Mol Pharm* 2012;**9**:260–80.

24. Nelson KM, Dahlin JL, Bisson J, Graham J, Pauli GF, Walters MA. The essential medicinal chemistry of curcumin. *J Med Chem* 2017;**60**:1620–37.

25. Naksuriya O, Okonogi S, Schiffelers RM, Hennink WE. Curcumin nanoformulations: a review of pharmaceutical properties and preclinical studies and clinical data related to cancer treatment. *Biomaterials* 2014;**35**:3365–83.

26. Allijn IE, Schiffelers RM, Storm G. Comparison of pharmaceutical nanoformulations for curcumin: enhancement of aqueous solubility and carrier retention. *Int J Pharm* 2016;**506**:407–13.

27. Du L, Feng X, Xiang X, Jin Y. Wound healing effect of an *in situ* forming hydrogel loading curcumin-phospholipid complex. *Curr Drug Del* 2016;**13**:76–82.

28. Sun Y, Du L, Liu Y, Li X, Li M, Jin Y, et al. Transdermal delivery of the *in situ* hydrogels of curcumin and its inclusion complexes of hydroxypropyl-β-cyclodextrin for melanoma treatment. *Int J Pharm* 2014;**469**:31–9.

29. Simon A, Amaro MI, Cabral LM, Healy AM, de Sousa VP. Development of a novel dry powder inhalation formulation for the delivery of rivastigmine hydrogen tartrate. *Int J Pharm* 2016;**501**:124–138.

30. Parumasivam T, Ashhurst AS, Nagalingam G, Britton WJ, Chan H-K. Inhalation of respirable crystalline rifapentine particles induces pulmonary inflammation. *Mol Pharm* 2017;**14**:328–35.

31. Lapsia S, Koganti S, Spadaro S, Rajapakse R, Chawla A, Bhaduri-McIntosh S. Anti-TNF-α therapy for inflammatory bowel diseases is associated with epstein-barr virus lytic activation. *J Med Virol* 2016;**88**:312–8.

32. Jiao D-m, Yan L, Wang L-s, Hu H-z, Tang X-l, Chen J, et al. Exploration of inhibitory mechanisms of curcumin in lung cancer metastasis using a miRNA-transcription factor-target gene network. *PLoS One* 2017;**12**:e0172470.

33. Jyoti K, Pandey RS, Kush P, Kaushik D, Jain UK, Madana J. Inhalable bioresponsive chitosan microspheres of doxorubicin and soluble curcumin augmented drug delivery in lung cancer cells. *Int J Biol Macromol* 2017;**98**:50–8.

34. Zhu W, Cromie MM, Cai Q, Lv T, Singh K, Gao W. Curcumin and vitamin E protect against adverse effects of benzo[*a*]pyrene in lung epithelial cells. *PLoS one* 2014;**9**:e92992.

35. Chang H-B, Chen B-H. Inhibition of lung cancer cells a549 and h460 by curcuminoid extracts and nanoemulsions prepared from *Curcuma longa* llinnaeus. *Int J Nanomed* 2015;**10**:5059–80.

36. Roy B, Guha P, Bhattarai R, Nahak P, Karmakar G, Chettri P, et al. Influence of lipid composition, pH, and temperature on physicochemical properties of liposomes with curcumin as model drug. *J Oleo Sci* 2016;**65**:399–411.

37. Price LC, Shao D, Meng C, Perros F, Garfield BE, Zhu J, et al. Dexamethasone induces apoptosis in pulmonary arterial smooth muscle cells. *Respir Res* 2015;**16**:114–30.

38. Ou Y-q, Zhu Wb, Li Y, Qiu P-x, Huang Y-j, Xie J, et al. Aspirin inhibits proliferation of gemcitabine-resistant human pancreatic cancer cells and augments gemcitabine-induced cytotoxicity. *Acta Pharmacol Sin* 2010;**31**:73–80.

39. Naykoo NA, Dil-Afroze, Rasool R, Shah S, Ahangar AG, Bhat IA, et al. Single nucleotide polymorphisms, haplotype association and tumour expression of the vascular endothelial growth factor (VEGF) gene with lung carcinoma. *Gene* 2017;**608**:95–102.

40. Fadus MC, Lau C, Bikhchandani J, Lynch HT. Curcumin: an age-old anti-inflammatory and anti-neoplastic agent. *J Trad Complement Med* 2017;**7**:339–46.

41. Toden S, Theiss AL, Wang X, Goel A. Essential turmeric oils enhance anti-inflammatory efficacy of curcumin in dextran sulfate sodium induced colitis. *Sci Rep* 2017;**7**:814–25.

42. Sandersen C, Bienzle D, Cerri S, Franck T, Derochette S, Neven P, et al. Effect of inhaled hydrosoluble curcumin on inflammatory markers in broncho-alveolar lavage fluid of horses with LPS-induced lung neutrophilia. *Multidiscip Respir Med* 2015;**10**:16–24.

43. Rashid K, Chowdhury S, Ghosh S, Sil PC. Curcumin attenuates oxidative stress induced NF-κB mediated inflammation and endoplasmic reticulum dependent apoptosis of splenocytes in diabetes. *Biochem Pharmacol* 2017;**143**:140–55.

44. Busch CJ, Binder CJ. Malondialdehyde epitopes as mediators of sterile inflammation. *Biochim Biophys Acta* 2017;**1862**:398–406.

45. Li J, Zhou Y, Zhang W, Bao C, Xie Z. Relief of oxidative stress and cardiomyocyte apoptosis by using curcumin nanoparticles. *Colloids Surf B Biointerfaces* 2017;**153**:174–82.

46. Patel HJ, Patel BM. TNF-α and cancer cachexia: molecular insights and clinical implications. *Life Sci* 2017;**170**:56–63.

47. Jiang W-W, Wang Q-H, Liao Y-J, Peng P, Xu M, Yin L-X. Effects of dexmedetomidine on TNF-α and interleukin-2 in serum of rats with severe craniocerebral injury. *BMC Anesthesiol* 2017;**17**:130–135.

48. Liu Y-h, Liu G-h, Mei J-j, Wang J. The preventive effects of hyperoside on lung cancer *in vitro* by inducing apoptosis and inhibiting proliferation through caspase-3 and p53 signaling pathway. *Biomed Pharmacother* 2016;**83**:381–91.

49. Zhang D, Zou Z, Ren W, Qian H, Cheng Q, Ji L, et al. Gambogic acid-loaded PEG-PCL nanoparticles act as an effective antitumor agent against gastric cancer. *Pharm Dev Tech* 2018;**23**:33–40.

50. Garner TP, Lopez A, Reyna DE, Spitz AZ, Gavathiotis E. Progress in targeting the BCL-2 family of proteins. *Curr Opin Chem Biol* 2017;**39**:133–42.

51. Liu B, Wang C, Chen P, Wang L, Cheng Y. Rack1 promotes radiation resistance in esophageal cancer *via* regulating Akt pathway and Bcl-2 expression. *Biochem Biophys Res Comm* 2017;**491**:622–8.

52. Huniadi CA, Pop OL, Antal TA, Stamatian F. The effects of ulipristal on Bax/Bcl-2, cytochrome C, Ki-67 and cyclooxygenase-2 expression in a rat model with surgically induced endometriosis. *Eur J Obst Gynecol Reprod Biol* 2013;**169**:360–5.